Dissolution of Whey Protein Concentrate Gels in Alkali

Ruben Mercadé-Prieto and Xiao Dong Chen
Dept. of Chemical and Materials Engineering, The University of Auckland, Private Bag 92019, Auckland, New Zealand

DOI 10.1002/aic.10639
Published online September 28, 2005 in Wiley InterScience (www.interscience.wiley.com).

The dissolution of whey protein concentrate (WPC) gels has been studied in detail, and the different mechanisms involved have been quantitatively analyzed. The NaOH diffusivity in gels has been determined at different pH at 22°C. Dissolution experiments of gels under several conditions have been performed and compared. Both heat-induced gels (HIG) and caustic-induced gels (CIG) have been studied as models to heat-exchanger fouling deposits. It is proposed that the constant dissolution rate observed at low pH is controlled by the reactions that break down the gel structure, particularly the β-elimination of intermolecular disulfide bonds. Alkali dissolution of CIG is reduced with increasing the gelation pH, as more crosslinks are present in the gel. It is proposed that a similar mechanism of crosslink formation may explain the low dissolution rates observed in HIG at dissolution pH above 13.1. NaOH diffusion is observed to limit the dissolution process at high temperatures and pH close to 13. © 2005 American Institute of Chemical Engineers *AIChE J,* 52: 792–803, 2006
Keywords: heat-induced gels, caustic-induced gels, dissolution rate, disulfide bonds β-elimination

Introduction

The fouling of process surfaces by whey proteins and associated fluids is of considerable importance in the dairy sector. Great advances have been made in the understanding of the cleaning of whey-fouled surfaces relative to cleaning-in-place (CIP) systems for the dairy industry. In the last decade, the emphasis has shifted to study of the dynamic behavior of the cleaning process using different techniques.[1-3] Recently, Xin et al.[4] have determined the cleaning rates through non-invasive UV spectrophotometric measurements at short intervals (5-10 s).

Continuous monitoring of the cleaning process has permitted the identification of three stages. In the first or swelling stage, the protein fouling deposits swell in contact with NaOH[3] before a uniform or plateau stage, where the cleaning rate remains relatively constant over time. Finally, in the decay stage, the cleaning rate slowly decreases to zero, suggesting that the deposit removal is complete.[2] For thick deposits the most important stage in the cleaning process is the plateau stage,[5] because this is where most of the foulant is removed. Xin et al.[4] obtained good agreement with a mass transfer controlled model, where the mass transfer coefficient in the gel boundary was calculated using standard correlations. However, as in other mass transfer models,[6,7] there is considerable uncertainty when estimating the values of WPC saturation concentration in the boundary layer. The problems discussed by LeClerq-Perlat and Lalande[8] in applying the mass transfer approach to explain the entire picture of a dissolution process have not yet been solved.

The chemical dissolution process can be briefly summarized in three steps, being a modified version of the mechanism proposed by Harper[9]:

(1) Diffusion of the NaOH from the bulk solution into the gel.

(2) Chemical reactions take place and bonds are broken.

(3) Unattached aggregates or proteins leave the gel through the boundary layer.

*Correspondence concerning this article should be addressed to X. D. Chen at d.chen@auckland.ac.nz

The aim of this study was to analyze each step in detail in order to assess the contribution of each to the overall dissolution process, and to elucidate the existence of an optimal NaOH concentration.

Experimental Procedures

NaOH diffusion

Experiments were performed to measure the penetration depth of NaOH into a heat-induced whey gel (HIG). Gels were formed inside small glass capsules, 5 mm internal diameter and 25 mm high, using a well homogenized 16.7 wt % WPC solution (~80% protein WPC, New Zealand Milk Products (NZMP)). Care was taken to avoid bubbles or foam in the solution. The sample was then sealed with foil and held in a water bath at 80°C for 20 minutes. A wire support held the capsule vertical during the gelation process. The capsules were then cooled down to, and held at, room temperature for at least half an hour before being inserted into a caustic solution (~200 ml) of known concentration. Capsules were kept in the vertical position and in contact with NaOH. At different times, the capsules were removed from the alkali solution, the gel surface dried with a tissue paper, a picture was taken with a digital camera, and the capsule was returned to the caustic solution; the whole process lasted a minute or less. The penetration depth of the caustic and the gel boundary were measured from one end of the tube, to an accuracy of ~0.2 mm. Even though the penetration depth could be measured unaided with normal whey gels, it was found that the resolution could be enhanced if some drops of phenolphtaleine (~0.1 g phenolphtaleine in 100 ml EtOH 95 wt %, a pH indicator in the 8.2-9.8 range) were added to the whey solution before gelation. Tests indicated that the phenolphtaleine did not affect the measurements within the limits of experimental error.

Dissolution of WPC gels

Heat-induced gels (HIG) were prepared using the procedure described above but without phenolphtaleine. The gelation temperature (T_{gel}) was varied between 75-95°C. The gels were used within 0.5 and 4 h after they were made, to minimize the effect of drying on the surface. Most of the gels were made from 16.7 wt % WPC at 80°C; these are termed standard HIG.

Caustic-induced gels (CIG) were also prepared by mixing known amounts of a mother whey solution, water, and concentrated NaOH solution (~4 M) in a test tube. After homogenization, the solution was introduced into capsules, sealed with foil, and submerged in a water bath at 50°C for 20 minutes, as in HIG preparation. Unless otherwise stated, the final WPC concentration was 16.9 wt %. The gelation pH (pH_{gel}) of the gel was calculated using the hydrogen ion equilibrium of WPC solutions.[10] If the gels were not used within half an hour after preparation, they were kept at 4°C to suppress any gelation reactions.

Figure 1 shows the experimental set up for dissolution experiments. 200 ml of deionized water or caustic solution (analytical grade) were added to a 250 mL Erlenmeyer. The Erlenmeyer was insulated and the temperature held constant to ±2°C. The pH was measured every experiment by titration of an aliquot with HCl 0.02N standard analytical grade. Once the solution reached the desired temperature, a blank was scanned

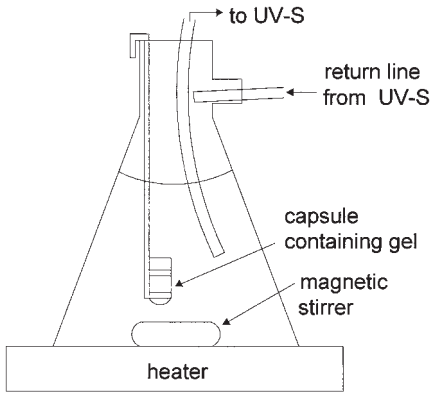

Figure 1. Gel dissolution experiments. UV-S: UV spectrophotometer.

Capsule dimensions: 5 mm internal diameter and 25 mm high.

with a UV diode array spectrophotometer (HP 8452A). More information on the continuous non-invasive UV measurements is given in Xin et al.[4] Finally, the capsule with the gel was suspended upright from the top of the Erlenmeyer with a wire and the spectrophotometer started to record. A small part of the solution was recirculated through the spectrophotometer and the UV absorption recorded at 30 s intervals.

Several wavelengths were used to determine the protein concentration in the solution. In alkali the wavelengths used were 224, 240, 250, and 280 nm, while for pure water 192 and 224 nm were used. The extinction coefficients were obtained for the pH range used. The use of several wavelengths has been found to improve significantly the stability and accuracy of the results across a wide range of protein concentration. The dissolution rate was then calculated using numerical three-point differences of the mean concentration. To partially eliminate the noise, rates were smoothed by calculating a moving average, with sample sizes of three if the rate is changing quickly (e.g., during the swelling stage), and up to 9 as it becomes more even (usually beyond 3000 s).

Mass transfer of loose proteins

The bulk of the dissolution experiments in this study were performed using a stirring speed of 350 rpm. To check if the amount of dissolved proteins formed was affected by the stirring velocity, dissolution experiments were also performed at the lowest speed setting, ~100 rpm. Figure 2 compares a typical experiment (350 rpm) and one where the stirring speed is switched periodically between 100 and 350 rpm. Lower dissolution rates were systematically found at 100 rpm; but when the stirring speed was increased to 350 rpm, a peak was always observed due to a sudden jump of the protein concentration in solution. The significant difference in the dissolution rate values (~20%) may indicate that the stirring speeds influence the dissolution rate. However, if the concentration increase seen during the peak is added to the dissolution rate seen in the 100 rpm period, the total quantity of loose proteins formed is the same as that when using 350 rpm. If the stirring velocity does influence the formation of loose proteins in the dissolution process, its effects are too small to be detected with

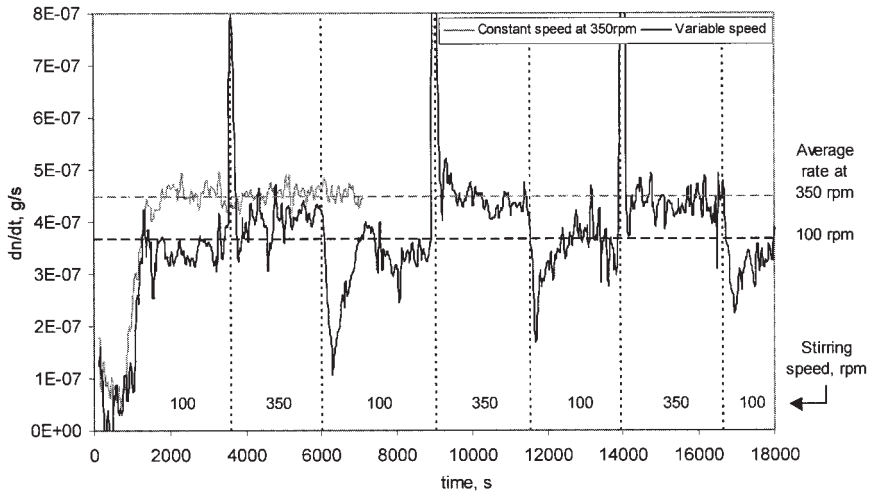

Figure 2. Effect of the stirring velocity on the dissolution rate for standard HIG with pH_{dis} 12.72 and 21°C.

The vertical lines indicate when the stirring velocity was changed.

the procedure used here, as the repeatability and the mean rates accuracy were not better than 5%.

Results

NaOH diffusion

The first step in the cleaning mechanism is the diffusion of NaOH into the deposit. The penetration of the NaOH is considered to be fast,[2,4] but no diffusivity measurements have been reported to verify its extent. Experiments have been conducted to measure the NaOH diffusivity in heat-induced gels, and the diffusivity was estimated as outlined in the Appendix. The typical agreement of the penetration depth profile is shown in Figure 3. The effective diffusivity values found for pH between 12 and 14 are shown in Figure 4. For comparison, the diffusivity values of NaOH in water are also shown. The apparent diffusivity minimum near pH 13 is suggested to be related to the extensive dissolution seen at those concentrations. This would decrease the effective NaOH concentration at the boundary, as the samples were not stirred, and hence the apparent diffusivity would be lower. Figure 4 indicates that an average diffusivity value of 1.1-1.3 $\times$ 10^{-9} m^2 s^{-1} at 22°C should be used for the whole range of normal cleaning concentrations (pH 12-13.7). By contrast, the apparent diffusivity of NaOH in potato flesh, containing about 80% water, is reported in the range of 0.8 to 1.1 $\times$ 10^{-9} m^2 s^{-1}.[11]

It is interesting to compare the experimental diffusivity values found with standard predictions. The diffusivity in porous materials is estimated using Eq. 1,[12] where D_{model} is the effective diffusivity, D is the diffusivity in a free medium, in water in this case, ε is the porosity, and τ is the tortuosity. The parameter ε is considered the water volume fraction in the gel, at ~0.91 (gel density of 1.1 g cm^{-3}[4]).

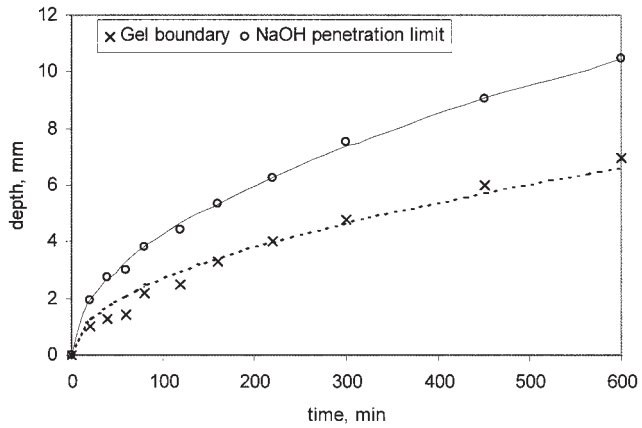

Figure 3. NaOH penetration depth at different times for a 16.7 wt% phenolphtaleine-labeled whey gel at pH 13.07 and 22°C from initial boundary position.

Continuous line: numerical simulation using D_{eff} = 9.6 $\times$ 10^{-10} m^2 s^{-1}; dashed line: calculated x_b using β_b = 1.74 $\times$ 10^{-5} m $s^{-0.5}$ (Eq. A1).

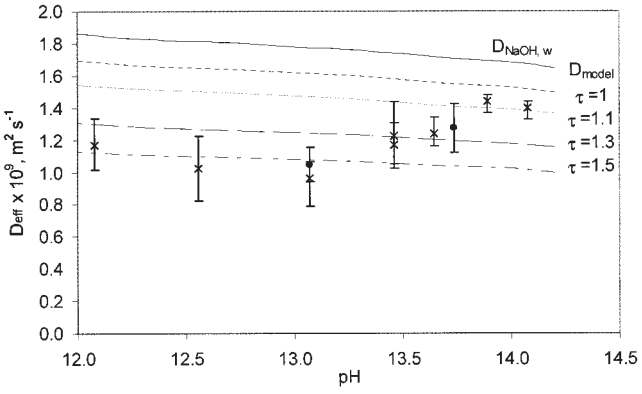

Figure 4. Effect of pH on NaOH effective diffusivity at 22°C.

Crosses: experimental values in 16.7 wt % HIG using phenolphtaleine; filled circles: without phenolphtaleine. The error bars correspond to the diffusivity values calculated using an NaOH concentration 5% different than the nominal, plus the standard deviation of the penetration depth and of β_b. D_{model} is the diffusivity in water[41]; and D_{model} lines are the calculated effective diffusivity in a gel (Eq. 1), using ε = 0.91 and different tortuosity τ values.

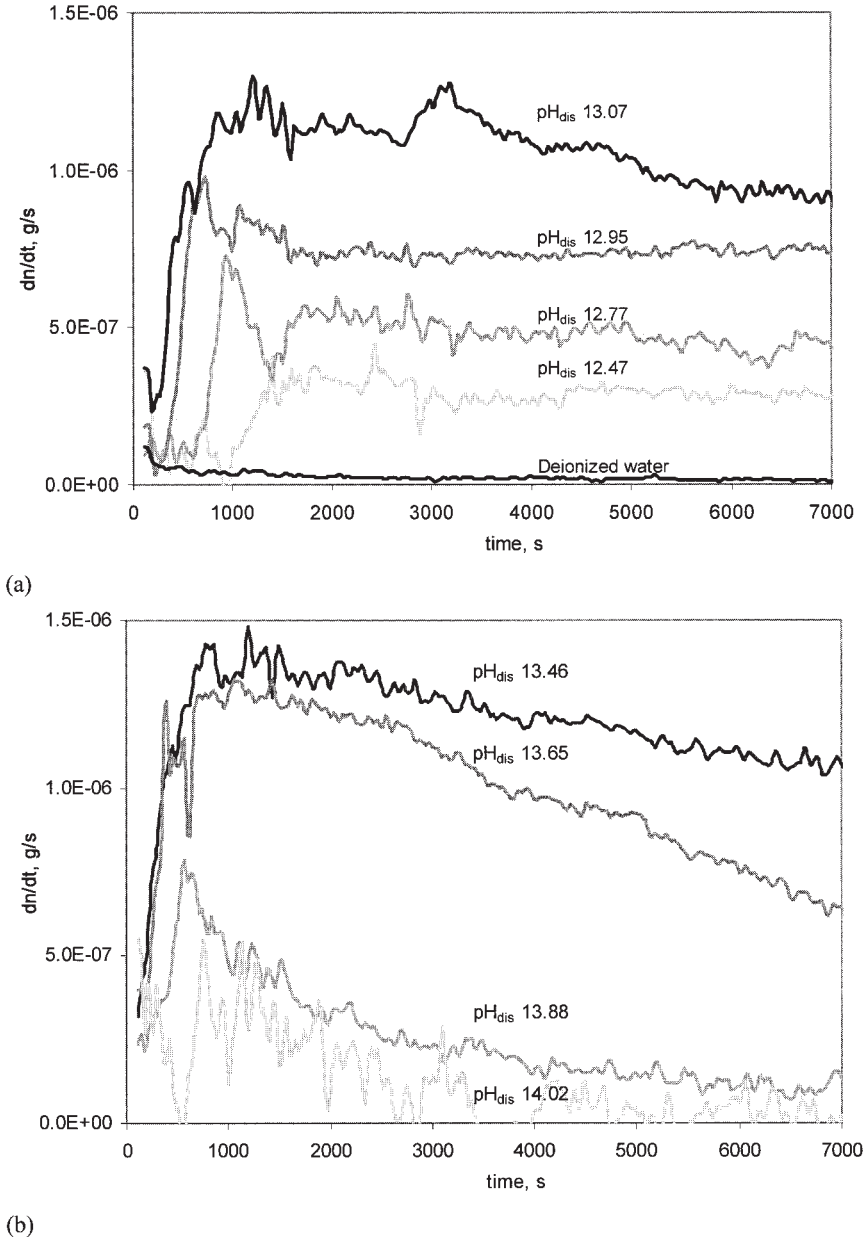

Figure 5. (a) Dissolution rate profiles at low pH_{dis}; (b) dissolution rate profiles at high pH_{dis} showing decreasing trend.
Conditions: standard HIG dissolved at 21°C.

The τ values obtained with three different correlations found in the literature[13] were 1.05, 1.10, and 1.31. Figure 4 shows the effective diffusivity estimated using different tortuosity values.

$$D_{model} = D \cdot \frac{\varepsilon}{\tau} \tag{1}$$

The diffusivity estimations reported in the literature for cleaning experiments have been somewhat rough, and the equations used simplify greatly the reality. Tuladhar et al.[3] suggested that "the diffusivity of NaOH through a protein would be a 'facilitated diffusion' wherein the OH- diffusivity is substantially larger than the above (5×10^{-9} m^2 s^{-1}) value." The values found in the present study clearly disagree with this proposition, as the diffusivity in a gel is about two thirds that in water. We also draw attention to the fact that the estimation of diffusivity via solutions to Fick's second law is not strictly appropriate to these dissolving gel systems. The hydroxide ions react with the protein, and the WPC hydrogen ion equilibrium has to be used. If these reactions had not been taken into account, the diffusivity values found would have been 20-40% lower than those shown in Figure 4. NaOH diffusion simulations at 22°C have shown that this is a fast step in the conditions studied, even though this cannot be assured for higher temperatures.

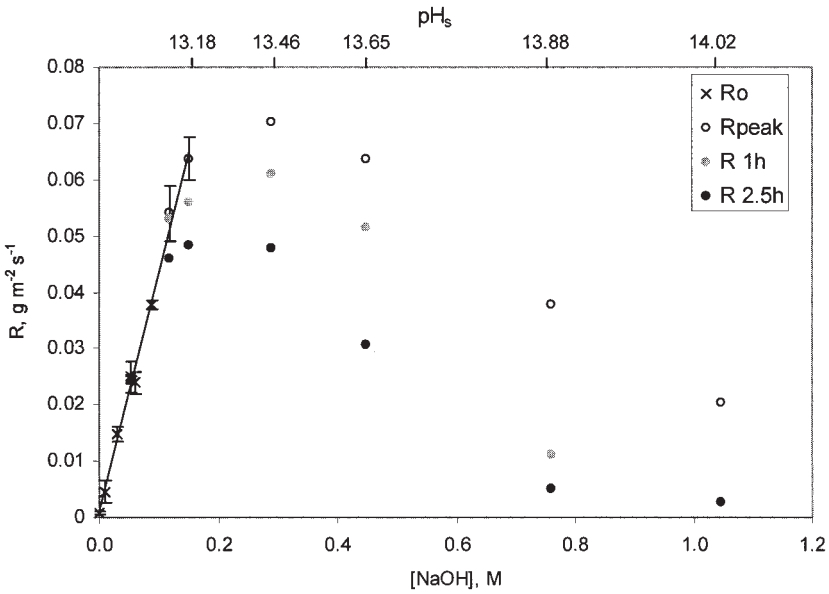

Figure 6. Dissolution rate per unit area for standard HIG at different dissolution NaOH concentrations at 21°C.

R_o refers to experiments exhibiting uniform dissolution rates, R_{peak} is the maximum rate found, and R_{1h} and $R_{2.5h}$ are the rates after 1 and 2.5 hours, respectively. The line is Eq. 2 with the best-fitted parameters for HIG.

Dissolution of heat-induced gels (HIG)

Influence of Dissolution pH. The effect of dissolution pH (pH_{dis}) was studied across the pH_{dis} range 12-14 and also with deionized water. Figure 5a shows that at low pH_{dis}, between 12 and 13, the dissolution rate starts from a small value and after a time it rises to a value that is effectively uniform with time (R_o). For standard HIG dissolved at room temperature and pH_{dis} 12.72, the R_o values found for three experiments agreed within 5%, and the standard error in each set of values was 10% or less, indicating that the uniform dissolution rate is reproducible and can be measured accurately. The constant dissolution rates observed are considered to represent the rate of a chemical reaction.[14] The dissolution produced by the presence of caustic is termed $R_{\beta E}$ in connection with the β-elimination of intermolecular disulfide bonds, which is the most likely reaction involved as discussed further on. Some dissolution is observed in deionized water due to the partial solubility of the WPC gels, and this is termed R_w. R_o can then be expressed with the following equation:

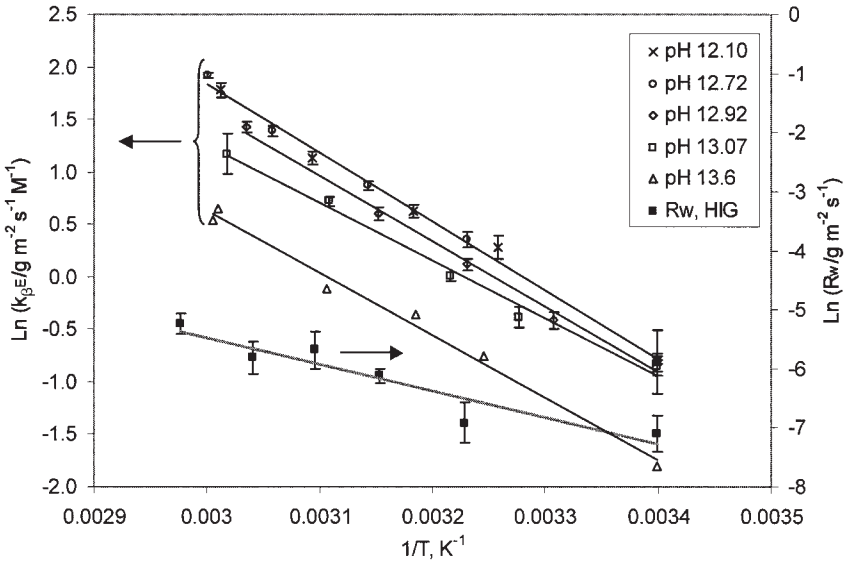

Figure 7. Arrhenius plots of R_w and $k_{\beta E}$ at various pH_{dis} for standard HIG. $k_{\beta E}$ is calculated using R_o in Eq. 3, except for pH_{dis} 13.6, where the maximum rate is used, R_{peak}.

Lines show results of linear regression. Calculated E_a: pH_{dis} 12.10, 53.8 kJ mol^{-1}; pH_{dis} 12.72, 55.6 kJ mol^{-1}; pH_{dis} 12.94, 51.7 kJ mol^{-1}; pH_{dis} 13.07, 45.6 kJ mol^{-1}; pH_{dis} 13.60, 51.1 kJ mol^{-1}.

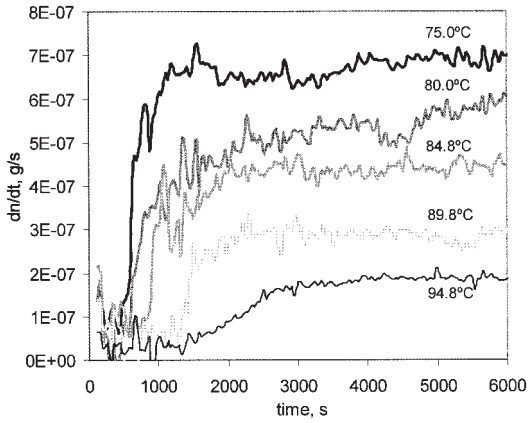

Figure 8. Dissolution rate profiles of standard HIG prepared at different gelation temperatures.

Conditions: pH_{dis} 12.72 and 21°C.

$$R_o = \frac{1}{A}\left(\frac{dn}{dt}\right)_{uniform} = R_{\beta E} + R_w = k_{\beta E}[OH^-]^{m_{\beta E}} + R_w \qquad (2)$$

where R_o is the average dissolution rate per unit area in the uniform stage, A is the exposed gel surface area, n is the protein dissolved, $(dn/dt)_{uniform}$ is the dissolution rate in the uniform stage, and $[OH^-]$ is the hydroxide concentration of the solution. Values of the parameters for standard HIG were as follows: rate constant, $k_{\beta E} = 0.46 \pm 0.01$ g m^{-2} s^{-1} M^{-1}; reaction order, $m_{\beta E} = 1.02 \pm 0.03$; and water-only dissolution rate, $R_w = (8 \pm 3) \times 10^{-4}$ g m^{-2} s^{-1}. The values have been found with a least squares method ($R^2 = 0.994$) up to an NaOH concentration of 0.15 M, and these data are plotted in Figure 6. The accuracy of R_w is low because little is dissolved and the signal to noise ratio in the UV spectrophotometer is small.

Dissolution experiments performed at pH_{dis} above 13 showed a significant decline in dissolution rate over the length of the experiments (Figure 5b). The uniform dissolution rate plateau is shorter lived at higher pH_{dis}, so that at pH_{dis} 13.88 and 14.02 there was just a peak. Furthermore, the peak values do not follow the trend in uniform rate suggested by Figure 6, as above pH_{dis} 13.2 the dissolution rate no longer increases with the NaOH concentration and above pH_{dis} 13.5 it decreases. In these latter experiments, the region of the gel attacked by the caustic experiences some color changes. At 21°C and $pH_{dis} \leq 13.5$, the caustic attacked phase is colorless. At higher hydroxide concentrations, a faint yellow color emerges in the attacked area; its brightness increases with pH_{dis} and temperature.

Influence of Dissolution Temperature. Eq. 2 features two temperature dependent parameters, $k_{\beta E}$ and R_w, which were modeled by Arrhenius dependencies, $E_{a,\ \beta E}$ and $E_{a,\ Rw}$, respectively, as shown in Figure 7. The activation energy found for pH_{dis} 12.10 and 12.72 is statistically the same and is considered to be the activation energy of the chemical reaction; the combined fit is shown in Figure 7. However, the E_a value found at pH_{dis} 12.92 and 13.07, when constant R_o is still observed, is smaller than those previous ones. Eq. 3 is the generalized version of Eq. 2 that includes the temperature effect, and the best-fitted parameters were as follows: $k_{\beta E,\ 0} = 2.38 \times 10^9$ g m^{-2} s^{-1} M^{-1}, $E_{a,\ \beta E} = 54.7 \pm 1.4$ kJ mol^{-1}, $R_{w,\ 0} = 3.58 \times 10^3$ g m^{-2} s^{-1}, and $E_{a,\ Rw} = 38 \pm 7$ kJ mol^{-1}.

$$R_o = k_{\beta E,0}e^{[-(E_{a,\beta E}/R_gT)]} \cdot [OH^-]^{1.0} + R_{w,0}e^{[-(E_{a,Rw}/R_gT)]} \qquad (3)$$

Dissolution of standard HIG at pH_{dis} 13.6, where the dissolution rate decreases with time, was also studied at different temperatures, but the results are complicated to interpret. At higher temperatures the maximum plateau (or peak) value increases, as observed at lower pH_{dis} (Figure 7). Between 20 and 40°C, increasing the temperature also provoked a faster decrease in the dissolution rate. For example, after one hour the dissolution rate for the experiments at 35 and 41°C was similar to the 21°C experiment. However, at 49°C, the rate decline was much less severe, and at 59°C the dissolution rate was so high that at the end of the experiment less than 10% of the original gel remained in the capsule.

Influence of Gelation Temperature. The gelation temperature for standard HIG gels was varied between 75 and 95°C. Figure 8 shows that the dissolution of these materials all exhibited uniform cleaning rate behavior. It is also noteworthy that increasing T_{gel} increases the time needed for the dissolution rate to reach its constant value.

Dissolution of caustic-induced gels (CIG)

Influence of Dissolution pH. The dissolution rate of CIG prepared at pH_{gel} 13.5 remains constant from pH 7 up to 13.6 at $1 \pm 0.3 \times 10^{-2}$ g m^{-2} s^{-1} (at 21°C). The rate increases slightly to 1.5×10^{-2} g m^{-2} s^{-1} at pH_{dis} 13.88-14.02. For CIG prepared at lower pH_{gel} values, the effect of dissolution pH_{dis} is very different (Figure 9). If the dissolution pH_{dis} is low, from 7 to ~12.3 for pH_{gel} 10.6, or up to ~12.8 for pH_{gel} 11.4, R_o

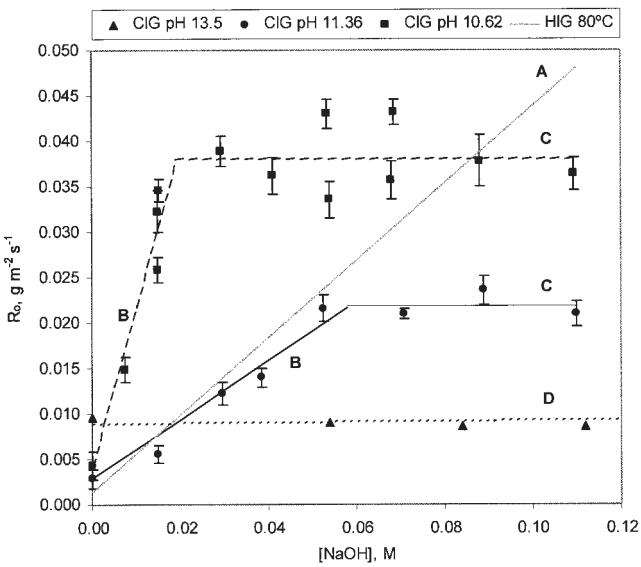

Figure 9. Effect of the dissolution NaOH concentration at 21°C on R_o for CIG gels prepared at different pH_{gel}.

(A) Dissolution by β-elimination of disulfide bonds for standard HIG, Eq. 2; (B) Dissolution by β-elimination of disulfide bonds for CIG, Eq. 2 and Table 1; (C) R_{limit} for different CIG; (D) Dissolution by solubility (R_w) for CIG pH_{gel} 13.5.

Table 1. Parameters for the Model in Eq. 2 for CIG Prepared at 16.9 wt % WPC, at 50°C for 20 Minutes

CIG pH_{gel} = 10.62	CIG pH_{gel} = 11.36
$7 < pH_{dis} < 12.3$	$7 < pH_{dis} < 12.8$
$k_{\beta E}(21°C) = 1.75 \pm 0.1$ g m^{-2} s^{-1} M^{-1}	$k_{\beta E}(21°C) = 0.32 \pm 0.02$ g m^{-2} s^{-1} M^{-1}
$R_w(21°C) = (4 \pm 1) \times 10^{-3}$ g m^{-2} s^{-1}	$R_w(21°C) = (3 \pm 1) \times 10^{-3}$ g m^{-2} s^{-1}

increases linearly with the hydroxide concentration. There is also a minimum value corresponding to the solubility effects in deionized water (R_w). A first order dependency on hydroxide concentration and the presence of a solubility value suggest that the dissolution seen at these pH_{dis} values is equivalent to that seen for HIG. Using the same notation as for HIG, the best values that represent this region using Eq. 2 are shown in Table 1. R_o above those pH_{dis} thresholds is, within experimental accuracy, constant. These constant values, which are the maximum R_o observed at each pH_{gel}, have been labeled R_{limit}. Figure 9 will be discussed in detail later.

Influence of Gelation pH. The dissolution rate for gels generated at a gelation pH (pH_{gel}) of 10 to 14 was examined using a dissolution pH_{dis} of 12.72 at 21°C. As seen previously for HIG, at this dissolution pH_{dis} and temperature, the dissolution rate was found to be uniform with time, but in these cases no time delay was seen and the dissolution rate quickly reached the constant value stage (Figure 10). Figure 11 shows the effect of pH_{gel} on R_o. R_o decreases when pH_{gel} is increased until ~12.6, after which it remains constant. Most probably, R_o stagnates around this pH_{gel} because the dissolution pH (12.72) is lower than the pH inside the gel. In this range of pH_{gel}, as discussed above for CIG prepared at pH_{gel} 13.5, the rate is the same as that for deionized water. We suggest that this dissolution rate should also be related to the solubility of the gel in water, like R_w, but now for a CIG made at very high pH_{gel}. R_o values shown in Figure 11 were obtained at pH_{dis} 12.72; therefore, the values below pH_{gel} ~11.4 correspond to R_{limit}, as the threshold pH $\leq pH_{dis}$ from Figure 9. The colors of the gels formed varied with the pH_{gel}. Below pH_{gel} 11.6, the gels were white and slightly transparent. Larger pH_{gel} yielded gels of yellow color, with the yellow color increasing in intensity with pH_{gel} (Figure 11).

Influence of Dissolution Temperature. The influence of temperature in the dissolution of CIG prepared at pH_{gel} 11.4 was investigated at three different pH_{dis}. At high temperatures, the dissolution rate decreased with time, and the remaining gels became more yellowish. For those experiments, R_o was chosen to be the plateau or the peak value seen at the beginning. The $E_{a,\ \beta E}$ values found were: 57.0 ± 2.2 kJ mol^{-1} at pH_{dis} 12.17, 43.7 ± 1.6 kJ mol^{-1} at pH_{dis} 12.72, and 57.3 ± 1.9 kJ mol^{-1} at pH_{dis} 13.06.

The temperature effect for the gels made at high pH_{gel} was also investigated. As reported before, the dissolution seen in this kind of gel is considered to occur mainly due to solubility effects. Therefore, R_o should be mainly independent of pH_{dis} (agreement not shown). The activation energy for R_w using several pH_{dis} (7-12.7) is 43 ± 3 kJ mol^{-1} for CIG pH_{gel} 13.5. However, experiments performed at high temperatures showed an unexpected dissolution rate behavior, as very high dissolution rate values were suddenly observed over a long period. For these experiments, visual observation of the capsules indicated that the gels had "collapsed," as only a liquid solution remained inside the capsules.

Discussion

Chemical reactions in HIG: the β-elimination of disulfide bonds

The relevance of intermolecular disulfide bonds in the formation of aggregates and larger oligomers has been widely reviewed.[15-17] Even though non-covalent bonds also play a role in the formation of HIG gels,[18] it has been recognized that for the kind of HIG generated here the main cohesive attractions are due to covalent disulfide bonds. Weak interactions are provably destroyed in the swelling stage by the electrostatic

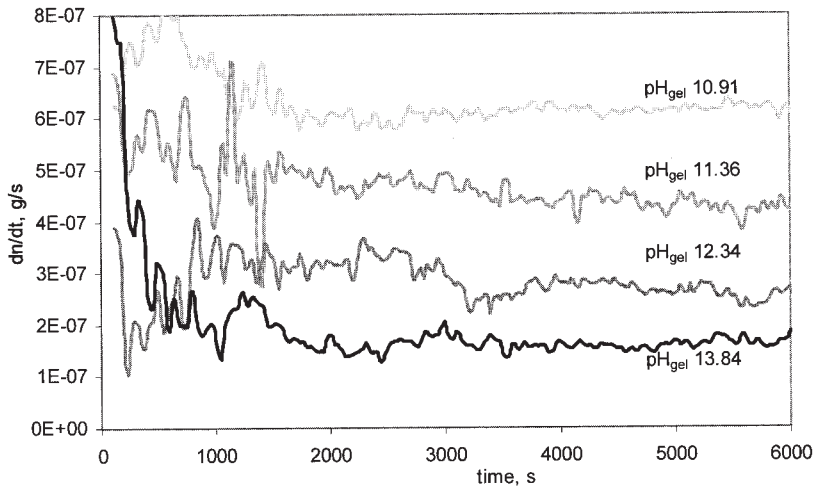

Figure 10. Dissolution rate profile for CIG generated at different gelation pH_{gel}. Conditions: pH_{dis} 12.72 at 21°C.

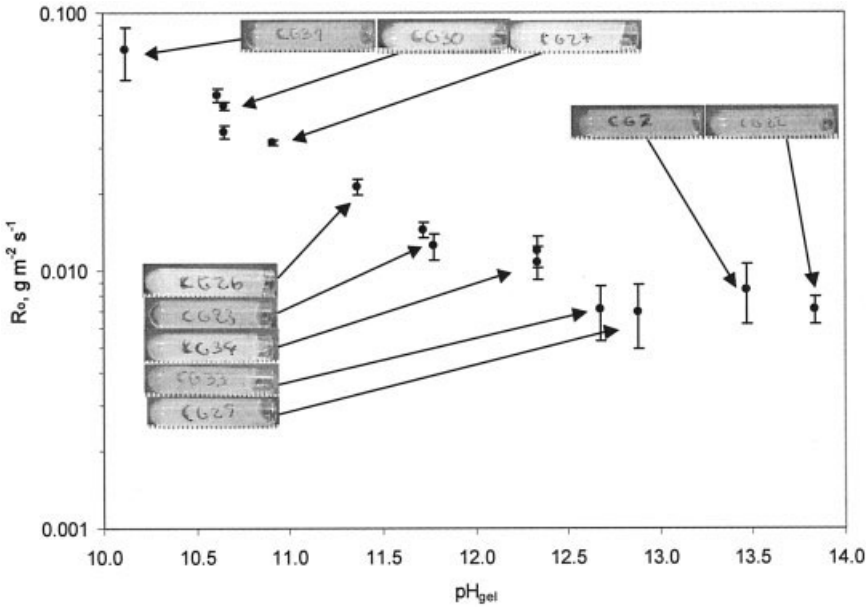

Figure 11. Effect of pH_{gel} on CIG dissolution.

Note log scale on y-axis. Images show the gels after gelation. Conditions: pH_{dis} 12.72 and 21°C.

repulsion after the NaOH diffusion. Therefore, in order to dissolve a gel completely, covalent bonds must be broken, namely the intermolecular disulfide bonds or the intramolecular peptide bonds. Chemical hydrolysis of the peptide bond requires harsh conditions,[19] whereas under the pH and the temperature conditions employed here, little evidence was found for the hydrolysis of ribonuclease A and lysozyme.[20]

Three mechanisms are recognized in the destruction of disulfide bonds, but only the β-elimination mechanism (Figure 12) has been widely verified,[21,22] even for β-lactoglobulin.[23] It is first order with respect to the hydroxide concentration,[24] in good agreement with the value found for $m_{\beta E}$. The activation energy found for the dissolution of HIG, $E_{a,\ \beta E}$ ~55 kJ mol^{-1}, is smaller but of the same order as that reported for the β-elimination of cystine residues in different proteins (60-100 kJ mol^{-1}).[25] The yellow color observed in HIG dissolved at high pH_{dis} and in CIG formed at high pH_{gel} is suggested to be due to the formation of organic and inorganic polysulphides from the β-elimination of disulfide bonds,[26] as when these gels were treated with acid, the yellowness disappeared and H_2S could be smelled.

Similar dissolution behavior to HIG is also seen for CIG (pH_{gel} 10.62 and 11.36) at low dissolution pH_{dis} (Figure 9). Although not as many experiments were performed as for HIG to confirm a first order dependency unequivocally, this trend fitted the experimental values well. In addition, the activation energy found at pH_{dis} 12.17 is statistically the same as for HIG (57 $\pm$ 3 kJ mol^{-1}). The present study, therefore, confirms those

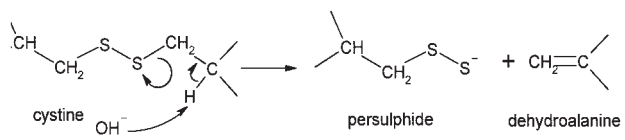

Figure 12. β-Elimination mechanism of disulfide bonds.

cleaning mechanisms based on a first order reaction with the hydroxide concentration, e.g., Jennings.[27]

Non-Constant dissolution rates

In the dissolution of HIG at high pH_{dis} it was shown in Figure 5b that two new phenomena occur: the dissolution rate decreases with time, and the peak dissolution rate seen doesn't follow Eq. 2. These observations are important as they define the existence of an optimum cleaning concentration. Figure 6 shows the rates measured at different NaOH concentrations at 21°C. Recently, Xin et al.[28] have proposed that the existence of an optimum concentration may be due to the formation of new covalent bonds at higher pH_{dis}, but there is little published evidence for this explanation other than their set of rheological measurements. The present study has found further evidence to confirm this hypothesis, and a new mechanism is proposed:

(1) A high NaOH concentration is needed for the caustic to diffuse quickly into the gel and to alkali denature the proteins.[29] Hidden disulfide bonds become more exposed, and the protein chains have greater mobility due to the formation of a swollen/transparent phase, even though it is still a gel.

(2) Cysteine residues that have not reacted during the heat-induced gelation are now more reactive and they can undergo thiol/disulfide interchange reactions with other protein bonds. Non-natural amino acid crosslinks from dehydroalanine may also be formed.

(3) The density of covalent crosslinks between proteins increases with time; meanwhile, the capacity of the caustic to break bonds is still the same. The rate of formation of loose proteins decreases with time.

(4) At long times, the gel structure in the transparent phase has been changed completely due to step (2), but due to the lack of reactants, no more crosslinking reactions take place. Therefore, the rate becomes constant with time.

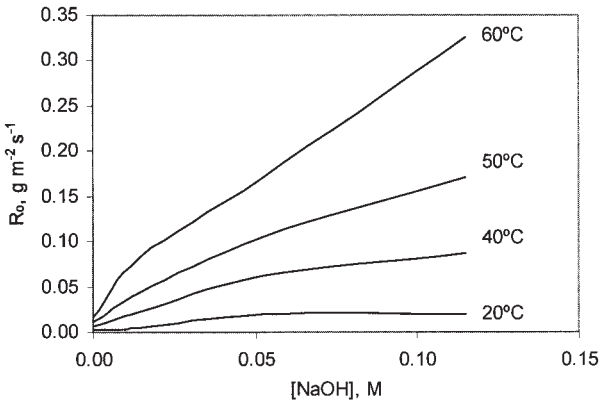

Figure 13. Calculated R_o at different pH_{dis} and temperatures for CIG pH_{gel} 11.36.

The role of the caustic in providing chemically stronger gels is seen in Figure 11. As the dissolution time increases, the NaOH concentration in the transparent phase increases. Once the high concentration needed for (1) is achieved (provably higher than pH 11-12), new intermolecular reactions (2) start to happen. Therefore, the time needed for (3) should be shorter at higher pH. Experimentally, the plateau peak values last less at higher pH, and at very high pH no plateau is observed, just a peak (Figure 5b). Finally, the crosslinking density in the gel cannot increase continuously, as the concentration of possible reactants is finite. When few new intermolecular bonds are formed with time, the dissolution rate will start to stagnate and, at the end, it will remain constant. This constant rate can be observed when using high pH_{dis} (13.88 and 14.02) as the rate decrease is fast. These final rates ($\sim 2 \times 10^{-3}$ g m^{-2} s^{-1}, Figure 5b) are similar to those small values found for CIG made at very high pH_{gel} (7-10 $\times 10^{-3}$ g m^{-2} s^{-1}, Figure 11). In addition, the gel color of HIG dissolved at those conditions resembles that found in the formation of CIG (see gel pictures at $pH_{gel} > 11.5$ in Figure 11). The mechanism proposed concludes that a normal HIG is transformed when dissolving at high pH_{dis} into a gel similar to a CIG.

Chemical reactions in CIG

Shimada and Cheftel[30] reported that increasing the gelation pH_{gel} from 6.5 to 9.5 resulted in gels that were easier to dissolve, as less hydrophobic and electrostatic interactions were involved. However, Figure 11 clearly shows that increasing the pH_{gel} above 10 R_o becomes smaller. As the electrostatic, hydrophobic, and hydrogen bonds are expected to be less relevant at higher pH_{gel}, the higher chemical resistance seen for CIG is explained in terms of more covalent bonds being present.[31] In the formation of CIG, a higher pH_{gel} yielded shorter gelation times.[10] It was suggested that NaOH enhanced thiol-disulfide interchange reactions. Therefore, for the same gelation time, the number of intermolecular disulfide bonds will increase with pH_{gel}. However, gelation times were seen to sharply increase above pH_{gel} 12.3-12.7. In addition, in this range of pH, a faint yellow color starts to emerge, which becomes more intense as the pH_{gel}, T_{gel}, and time increase. This color change may suggest that more disulfide bonds are being destroyed at high pH_{gel}, as discussed above.

If the destruction of disulfide bonds is enhanced at higher pH_{gel}, compared to the formation of new intermolecular bonds, this will result in there being an NaOH concentration where the net formation of bonds is maximum. This concentration is seen in gelation experiments, as the gelation time is a minimum at $pH_{gel} \sim 12.3$ at 50°C, and above this concentration much longer gelation times are needed.[10] However, it is not the case in the dissolution experiments, as R_o is not seen to increase at very high pH_{gel}. For gels made at high pH_{gel} and dissolved at high pH_{dis}, the R_o values found are very small, and they suggest that R_{limit} does not increase up to the pH_{gel} studied. This analysis suggests that crosslinks other than disulfide bonds have to be involved to keep the dissolution rate low.

To our knowledge, the only feasible crosslinks that can be formed in alkali treated proteins other than disulfide bonds are due to nucleophilic addition of dehydroalanine (DHA) residues. Many protein-bounded amino acids can react with DHA, like lysine and cysteine forming lysinoalanine (LAL) and lanthionine (LAN), respectively.[21] Although initial studies considered that most of these new bonds formed were intramolecular,[32] it has been shown that they can also be formed between proteins.[33-35] Several studies have reported for similar alkali conditions as those used here, a fast decline of the cystine content followed by an increase of LAL and LAN.[25,35,36]

Formation of new bonds in CIG made at mild alkali pH_{gel}

One issue that arises is that if at high pH_{gel} these new covalent bonds may be so important, how relevant are they at lower pH_{gel}? Figure 9 makes clear that the β-elimination mechanism cannot explain the whole trend in R_o with the hydroxide concentration. At low pH_{dis} it can be described as first order in [OH-] but then becomes zeroth order up to $pH_{dis} \sim 13$, the maximum studied. It should be emphasized that the dissolution rate is also uniform over time in this range of pH_{dis}. The analysis at higher temperatures yields new insights as the zeroth order observed is questioned (Figure 13). The stagnation seen at 20°C disappears at higher temperatures. We suggest that a new reaction takes place at these hydroxide concentrations with a kinetic constant too small to be determined at room temperature yielding the zeroth order observed. This reaction could be the destruction of LAL and LAN formed during gelation. It is known that high temperatures are needed to destroy these kind of bonds in alkali.[37,38]

Dissolution activation energy

The caustic penetration depth in standard HIG after 2 h in different dissolution conditions (conditions used in Figure 7) was measured as described in the diffusion experiments; results are shown in Figure 14. At low dissolution pH_{dis} (12.10 and 12.72) the penetration depth observed becomes smaller when increasing the temperature at all temperatures studied. This observation is expected, as the activation energy of the dissolution process, $E_{a,\beta E}$, is larger than that of the diffusivity. For pH_{dis} near the so-called "concentration optimum" (13.1 or 0.5 wt % NaOH[1]), the penetration depth also decreases at low temperatures, but above 35°C it stagnates at 1.4-1.5 mm. If the penetration depth does not decrease with the temperature, it suggests that diffusion of the caustic beyond this constant penetration depth is as fast as the chemical reactions to dissolve

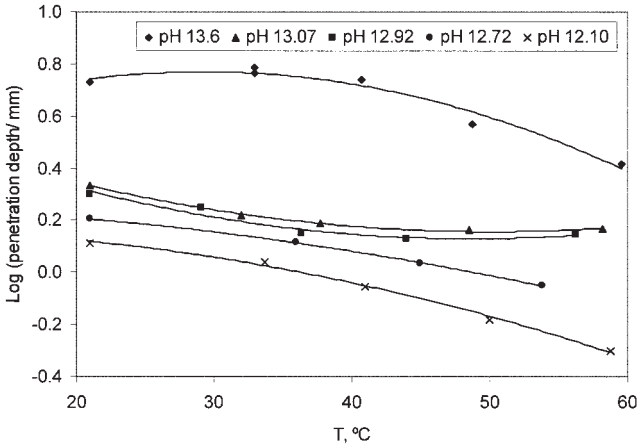

Figure 14. Logarithm of the NaOH penetration depth after dissolution experiments carried out for 2 hours at different pH_{dis} and temperatures for standard HIG (Figure 7).

The lines serve to guide the eye.

the gel. NaOH diffusivity simulations confirmed it. Hence, the overall process is not just controlled by the chemical reaction, as it is at low pH_{dis}, but it is determined by both the chemical reactions and the NaOH diffusion process. The increasing influence of the NaOH diffusion at higher pH_{dis} and higher temperatures will be reflected in a smaller apparent activation energy (in analogy to processes with high Hatta numbers[39]). We suggest that the lower activation energy seen for pH_{dis} 12.92 and 13.07 (51.7 and 45.6 kJ mol^{-1}, respectively, compared to 54.7 kJ mol^{-1} at lower pH_{dis}) is related to the increasing influence of NaOH diffusion.

Influence of the flow velocity in the cleaning process

Even though the influence of flow velocity has not been explicitly studied in this work, it is of interest to compare the values found here with those in the literature. The cleaning rate in pipes at different velocities reported by Xin et al.[5] is shown in Figure 15. A linear extrapolation of the data predicts a non-zero cleaning rate at zero flow velocity. Other studies show the same trend.[1-3] The HIG used here can be compared with the fouled pipes used by Xin et al.[5] as the WPC used was the same and the gelation conditions were similar. The calculated R_o for the same dissolution conditions is shown in Figure 15 (filled square) assuming zero flow velocity, as the formation of loose proteins was not enhanced by the stirring speed used. The extrapolation of Xin et al.'s data in pipes at zero velocity is in good agreement with the value found in the present study using a capsule. The present study supports the experimental evidence that at the limit of zero fluid velocity, the cleaning rate is non-zero. Flow velocity or shear stress does not affect the chemical reactions that produce loose proteins. They affect the transport (thus removal) of loose proteins from deposit to the bulk stream.

The results from this study are difficult to explain if the controlling mechanism is the mass transfer of unattached proteins. For example, how can the gelation parameters T_{gel} (Figure 8) or pH_{gel} (Figure 11) influence so greatly R_o at an appropriate shear rate (induced at 350 rpm) if the limiting mechanism is the boundary layer? Furthermore, the non-zero dissolution rate at zero velocity (extrapolated) could also be an indication of the working of the internal reactions. The first mechanism for cleaning must be the reactions that break down the gel structure. Whether or not the broken down gel particles or "dissolved" proteins can be removed (cleaned) from the deposit is facilitated by the fluid movement. As such, these reactions within the gel can become the limiting mechanism. Furthermore, the "dissolution" process, as we have observed, may also involve the removal of "particles or clusters" that could be further disintegrated in the cleaning solution. The generation of such particles or clusters are to do with the crosslink density (and the distribution of the crosslink density within the gel sample). When the crosslink density is low at certain spots inside a sample being subjected to the chemical solution, the bonds at these spots may be broken, which is sufficient to make loose clusters or lumps of protein that can be detached from the sample. This is a subject of continuing research.

Conclusions

Based on the current experimentation and analysis, it has been suggested that the chemical reactions that destroy the interprotein crosslinks are the most likely limiting mechanism in the "dissolution" of WPC gels. Moreover, the diffusion of NaOH into the gels should also be taken into account when the cleaning rate is very high. Strong evidence supports that the reactions seen in HIG are the β-elimination of intermolecular disulfide bonds. The dissolution rate decline in HIG when using high pH_{dis} has been analyzed as a transformation of the gels into CIG. Gels made at very high pH_{gel} present a significant chemical resistance to alkali. It has been proposed that new intermolecular crosslinks may provide the chemical resistance seen in CIG or in HIG dissolved at high pH_{dis}. Therefore, more conclusively than previous studies, an optimum pH_{dis} exists, beyond which the dissolution rate decreases with time.

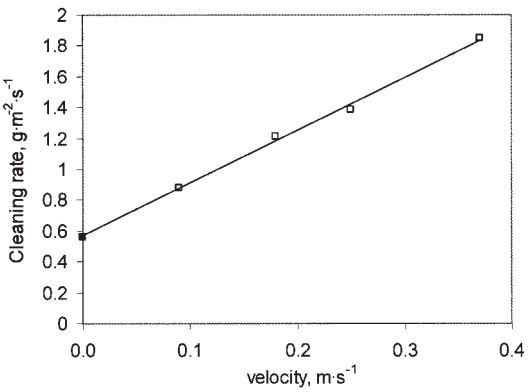

Figure 15. Influence of the velocity in the cleaning rate in pipes fouled with WPC gels.

The empty square points and line are after Xin et al.,[5] 0.5 wt % NaOH at 65°C. The black square is the calculated R_o for a standard HIG dissolved at the same conditions as Xin et al.'s data, assuming zero velocity.

Notation

A = exposed gel surface area, m^2
D = diffusivity in a free medium, $m^2\ s^{-1}$
D_{eff} = effective diffusivity in a porous media, $m^2\ s^{-1}$
D_{model} = effective diffusivity calculated by Eq. 1, $m^2\ s^{-1}$
dn/dt = dissolution rate, $g\ s^{-1}$
$E_{a,\ \beta E}$ = β-elimination activation energy, kJ mol^{-1}
$E_{a,\ Rw}$ = water solubility activation energy, kJ mol^{-1}
$k_{\beta E}$ = β-elimination rate constant, $g\ m^{-2}\ s^{-1}\ M^{-1}$
$m_{\beta E}$ = reaction order with respect to the NaOH concentration
n = protein dissolved, g
$[OH^-]$ = hydroxide concentration of the solution, M
pH_{dis} = dissolution pH
pH_{gel} = gelation pH
R^2 = regression coefficient
R = dissolution rate per unit area = $A^{-1}(dn/dt)$, $g\ m^{-2}\ s^{-1}$
$R_{\beta E}$ = β-elimination dissolution rate per unit area, $g\ m^{-2}\ s^{-1}$
R_g = ideal gas constant, $J\ mol^{-1}\ K^{-1}$
R_{limit} = maximum R_o observed for CIG, $g\ m^{-2}\ s^{-1}$
R_o = constant dissolution rate per unit area in the uniform stage, $g\ m^{-2}\ s^{-1}$
R_w = water solubility dissolution rate per unit area, $g\ m^{-2}\ s^{-1}$
t = time, s
T = temperature, K
T_{gel} = gelation temperature, °C
x_b = distance of the gel boundary from the initial position, m

Greek letters

β_b = gel-solution boundary parameter, $m\ s^{-0.5}$
ε = porosity of the solid, −
τ = tortuosity, −

Acronyms and abbreviations

CIG = caustic-induced gel
DHA = dehydroalanine
HIG = heat-induced gel
LAL = lysinoalanine
LAN = lanthionine
WPC = whey protein concentrate

Acknowledgments

The authors would like to thank Dr. D. I. Wilson for helpful discussion and critical input.

Literature Cited

1. Bird MR, Fryer PJ. An experimental study of the cleaning of surfaces fouled by whey proteins. *Trans IChemE, Part C, Food Bioprod Proc.* 1991;69:13-21.
2. Gillham CR, Fryer PJ, Hasting APM, Wilson DI. Cleaning-in-place of whey protein fouling deposits: mechanisms controlling cleaning. *Trans IChemE, Part C, Food Bioprod Proc.* 1999;77:127-136.
3. Tuladhar TR, Paterson WR, Wilson DI. Investigation of alkaline cleaning-in-place of whey protein deposits using dynamic gauging. *Trans IChemE, Part C, Food Bioprod Proc.* 2002;80:199-214.
4. Xin H, Chen XD, Özkan N. Cleaning rate in the uniform cleaning stage for whey protein gel deposits. *Trans IChemE, Part C, Food Bioprod Proc.* 2002;80:240-246.
5. Xin H, Chen XD, Özkan N. Removal of a model protein foulant from metal surfaces. *AIChE J.* 2004;50:1961-1973.
6. Schlussler HJ. Kinetics of the cleaning action on hard surfaces. *Brauwissenschaft.* 1976;29:263-276.
7. Gallot-Lavallée T, Lalande M. A mechanistic approach of pasteurised milk deposit cleaning. In: Lund DB, Plett E, Sandu C. (eds.), *Proc. of the 2nd Int. Conf. on Fouling and Cleaning in Food Processing*. Madison, WI, 1985:374-394.
8. Leclerq-Perlat MN, Lalande M. A review on the modelling of the removal of porous contaminants deposited in heat transfer surfaces. *Int Chem Engng.* 1991;31:74-93.
9. Harper WJ. Sanitation in dairy food plants. In: Gothie RK. (ed.) *Food Sanitation*. Westport, CT: The Avi. Publ. Co., Inc, 1972;130-160.
10. Mercadé-Prieto R, Chen XD. Caustic-induced gelation of whey deposits in the alkali cleaning of membranes. *J Membr Sci.* 2005;254: 157-167.
11. Chavez MS, Luna JA, Garrote RL. Apparent diffusion coefficient determination of NaOH through potato skin and flesh under different temperature and concentration conditions. *J Food Engng.* 1996;30: 377-388.
12. Knudsen JG, Hottel HC, Sarofim AF, Wankat PC, Kneabel KS. Heat and mass transfer. In: Perry RH, Green DW, Maloney JO (eds.). *Perry's Chemical Engineers' Handbook*. New York: McGraw-Hill International; 1997:5.55.
13. LeVan MD, Carta G, Yan CM. Absorption and ion exchange. In: Perry RH, Green DW, Maloney JO. *Perry's Chemical Engineers' Handbook*. McGraw-Hill International; 1997:16.19.
14. Jennings WG. Circulation cleaning. III. The kinetics of a simple detergent system. *J Dairy Sci.* 1959;42:1763-1771.
15. Surroca Y, Haverkamp J, Heck AJR. Towards the understanding of molecular mechanism in the early stages of heat-induced aggregation of β-lactoglobulin AB. *J Chromatogr A.* 2002;970:275-285.
16. Shimada K, Cheftel JC. Sulfhydyl group/disulfide bond interchange reactions during heat-induced gelation of whey protein isolate. *J Agric Food Chem.* 1989;37:161-168.
17. Hoffmann MAM, Van Mil PJJM. Heat-induced aggregation of β-lactoglobulin as a function of pH. *J Agric Food Chem.* 1999;47:1898-1905.
18. Havea P, Carr AJ, Creamer LK. The roles of disulphide and noncovalent bonding in the functional properties of heat-induced whey protein gels. *J Dairy Res.* 2004;71:330-339.
19. Bezkorovainy A. *Basic Protein Chemistry*. Springfield, IL: Charles Thomas; 1970.
20. Hayashi R, Kameda I. Conditions for lysinoalanine formation during exposure of protein to alkali. *Agric Biol Chem.* 1980;44:175-181.
21. Whitaker JR, Feeney RE. Chemical and physical modification of proteins by the hydroxide ion. *Crit Rev Food Sci Nutr.* 1983;19:173-212.
22. Kim JS, Kim HJ. Matrix-assisted laser desorption/ionization time-of-flight mass spectrometric observation of a peptide triplet induced by thermal cleavage of cystine. *Rapid Commun Mass Spectrom.* 2001;15: 2296-2300.
23. Noetzold H, Schlegel B, Tinius I, Freimuth U. Comparative amperometric and polarographic measurements of alkaline-treated β-lactoglobulin. *Zeitschrift fuer Chemie.* 1972;12:24.
24. Florence TM. Cathodic stripping voltammetry. Part II. Study of the release of inorganic sulfide from proteins during denaturation in alkaline media. *J Electroanal Chem.* 1979;97:237-255.
25. Feeney RE, Nashef AS, Osuga DT, Lee HS, Ahmed AI, Whitaker JR. Effects of alkali on proteins. Disulfides and their products. *J Agric Food Chem.* 1977;25:245-251.
26. Stapleton IW, Swan JM. Amino acids and peptides. VI. Studies on cystine and α,α'-dimethylcystine in relation to the alkaline degradation of protein disulfides. *Aust J Chem.* 1960;13:416-425.
27. Jennings WG. Theory and practice of hard surface cleaning. *Adv Food Res.* 1965;14:388-419.
28. Xin H, Chen XD, Özkan N. Whey protein-based gel as a model material for studying initial cleaning mechanisms of milk fouling. *J Food Sci.* 2002;67:2702-2711.
29. Taulier N, Chalikian TV. Characterization of pH-induced transitions of β-lactoglobulin: ultrasonic, densimetric, and spectroscopic studies. *J Mol Biol.* 2001;314:873-889.
30. Shimada K, Cheftel JC. Texture characteristics, protein solubility, and sulfhydryl group/disulfide bond contents of heat-induced gels of whey protein isolate. *J Agric Food Chem.* 1988;36:1018-1025.
31. Monahan FJ, German JB, Kinsella E. Effect of pH and temperature on protein unfolding and thiol/disulfide interchange reactions during heat-induced gelation of whey proteins. *J Agric Food Chem.* 1995;43:46-52.
32. Bohak Z. N-(DL-2-amino-2-carboxyethyl)-L-lysine, a new amino acid formed on alkaline treatment of proteins. *J Biol Chem.* 1964;239:2878-2887.
33. Correia JJ, Lipscomb LD, Lobert S. Nondisulfide crosslinking and chemical cleavage of tubulin subunits: pH and temperature dependence. *Arch Biochem Biophys.* 1983;300:105-114.

34. Chang JY. Stability of hirudin, a thrombin-specific inhibitor. *J Biol Chem.* 1991;266:10839-10843.
35. Karayiannis NI, MacGregor JT, Bjeldanes LF. Lysinoalanine formation in alkali-treated proteins and model peptides. *Food Cosmet Toxicol.* 1979;17:585-590.
36. Noetzold H, Schlegel B, Galani D. Alkali treatment of sulfhydryl and disulfide groups in alkali. *Nahrung.* 1977;21:697-704.
37. Friedman F, Levin CE, Norma AT. Factors governing lysinoalanine formation in soy proteins. *J Food Sci.* 1984;49:1282-1288.
38. Creamer LK, Matheson AR. Action of alkali on casein. *N Z J Dairy Sci Technol.* 1977;12:253-259.
39. Trambouze P, Van Landeghem H, Wauquier JP. *Chemical Reactors. Design, Engineering, Operation*. Houston, TX: Gulf Publishing Company; 1998.
40. Crank J. *The Mathematics of Diffusion*. Oxford, U.K.: Clarendon Press; 1998.
41. Bruins HR. Coefficients of diffusion in liquids. In: Washburn EW. (ed.), *International Critical Tables of Numerical Data, Physics, Chemistry and Technology*. Norwich, NY: Knovel, 2003:63-72.

Appendix: Estimation of NaOH Diffusivity

In order to calculate the apparent NaOH diffusivity in HIG when acid-base reactions also take place, Fick's first law was solved numerically at different length and time intervals, as described by Crank.[40] Part of the caustic that has diffused in a time interval will react with the proteins, resulting in a lower hydroxide concentration than that calculated with Fick's first law. The final concentration was calculated every time and length interval using the hydrogen ion equilibrium found in WPC solutions.[10] The effect of the moving boundary was included when the different depths were checked at each time interval with respect to the boundary gel-solution position, x_b. If the gel boundary is beyond the checked position at that time, the concentration is the one of the caustic solution. x_b is estimated with Eq. A1, where β_b is a parameter adjusted experimentally (Figure 3, dashed line). The experiments performed at a pH near 13 have large β_b values; meanwhile, if the dissolution pH is very small ($\sim$12) or very high ($\sim$14), negligible dissolution is seen and β_b equals zero.

$$x_b = 2\beta_b\sqrt{t} \tag{A1}$$

On suggesting a D_{eff} value, it is possible to perform the numerical simulation. Thereafter, the penetration depth at different times where the pH is 9.8 is found, when the phenolphtaleine has a bright pink color as seen in the gels. The penetration depth at the phenolphtaleine threshold is compared with the experimental values, and finally, by mean squares the D_{eff} that yields the best agreement is found (Figure 3, continuous line).

Manuscript received Feb. 15, 2005, and revision received Jun. 20, 2005.